Anti-Eavesdropping and Anti-Jamming Link with SPP Horn Antenna Based on Orbital Angular Momentum

Amir Habibi Daronkola[1], Farzad Tavakol Hamedani[1*] and Pejman Rezaei[1]

1. Faculty of Electrical and Computer Engineering, Semnan University, Semnan, Iran.ftavakkol@semnan.ac.ir

***Abstract*--This paper presents the design and development of a horn antenna with a spiral phase plate (SPP) for generating and utilizing orbital angular momentum (OAM) waves to enhance the security and capacity of communication links. OAM waves, with their unique properties such as increased spectral efficiency and channel capacity, as well as inherent resistance to eavesdropping and intentional jamming, have emerged as a novel and effective approach in telecommunications. In this research, three simulation scenarios at a frequency of 2.4 GHz are explored to evaluate the performance and security of OAM-based communication links. These scenarios include conventional and OAM-based links, with a specific focus on the second scenario where a jammer is positioned in the worst-case scenario—directly in front of the receiver antenna—to maximize the potential for link disruption. The simulation results demonstrate that by precisely tuning the parameters of the SPP, different OAM modes can be generated, which significantly hinder unauthorized access and signal degradation in communication links. Even under these challenging conditions, the proposed design achieved up to a 23.45 dB reduction in jammer signal strength, highlighting its robustness in enhancing link security and performance. This study not only shows that OAM-based links can boost the capacity and security of communication in 5G and 6G networks but also provides practical solutions for addressing security and interference challenges in modern communication systems.**

Index Terms: Orbital Angular Momentum (OAM); Horn Antenna; Spiral Phase Plate; Communication Security; OAM Mode.

I. INTRODUCTION

The rapid growth of the industry has led to the widespread adoption of innovative telecommunications solutions across various industries [1-3]. This has resulted in a significant enhancement of communication system performance and has opened up a new frontier for research and innovation in the field of telecommunications.

In recent years, researchers and scientists in the field of telecommunications have focused on improving key performance indicators for wireless communications. These key performance indicators include spectral efficiency [4-6], communication security [7-9], data rate [10-12], and the proliferation of the Internet of Everything (IoE) [13]. Enhancing these indicators plays a crucial role in transforming every aspect of human life.

With the ever-increasing advances in telecommunications and the widespread need for communication tools in everyday life, the telecommunications industry faces the challenge of frequency band congestion. Researchers are striving to develop new techniques to improve spectral efficiency. One common technique to reduce interference between communication systems in crowded environments involves various bandwidth management methods, such as improving the characteristics and performance of filters, duplexers, and other components [14-20]. In addition to conventional bandwidth management techniques, spatial management is employed to increase degrees of freedom, which helps prevent interference and expand available bandwidth.

One of the innovative methods for increasing the spatial degrees of freedom is the use of Orbital Angular Momentum (OAM) technology. OAM provides a new dimension for data transmission by utilizing helical phase wavefronts. This additional degree of freedom allows multiple independent data streams to be transmitted simultaneously over the same frequency band without interference, significantly increasing spectral efficiency and system capacity. The orthogonality between OAM modes further facilitates interference prevention, making it a promising solution for addressing frequency congestion in modern communication networks.

In early 1992, a groundbreaking discovery in the realm of light science revealed a hidden property: its ability to carry OAM, characterized by a twisting phase front [21]. This unique characteristic enables the simultaneous transmission of multiple radio beams with distinct helical phase fronts. The degree of twist in each beam's phase front defines its OAM mode, and these modes are orthogonal, allowing for seamless coexistence. This remarkable feature holds immense potential for enhancing the channel capacity and spectral efficiency of radio wave-based communication links.

Pioneering studies have demonstrated the feasibility of achieving a 32 Gbit/s radio link with a spectral efficiency of 16 bit/sHz using OAM-carrying waves in two polarizations [22]. The primary advantage of OAM-based communication lies in the inherent orthogonality between different OAM modes. This orthogonality expands the number of usable channels, significantly boosting the overall system capacity.

Compared to spin angular momentum (SAM), which offers only two orthogonal states, OAM presents a transformative approach to communication links, opening up exciting possibilities in various fields, including industry and academia [23]. Recent research has harnessed this principle in the optical domain, successfully combining multiple OAM modes to achieve remarkable capacity enhancements in free-space and fiber-optic communications, reaching terabit-per-second transmission rates [24,25].

Given the fundamental parallels between electromagnetic waves and light, it is natural to extend this OAM-based approach to the radio frequency regime [26]. By exploiting the unique properties of OAM, we can revolutionize radio communications, paving the way for a new era of high-capacity, secure, and reliable wireless connectivity.

OAM has emerged as a transformative technology with the potential to significantly enhance the capacity and spectral efficiency of radio communication links. However, the practical implementation of OAM-based systems faces a significant hurdle: the efficient multiplexing and demultiplexing of OAM modes [27]. While spatial light modulators (SLMs) have demonstrated remarkable effectiveness in manipulating OAM modes within the optical domain, facilitating efficient multiplexing and demultiplexing, directly translating this technology to the radio frequency regime presents significant challenges. These challenges stem from the inherent differences between light and radio waves [28].

The inherent advantage of boosting communication link capacity and spectral efficiency presents a significant challenge when translating this technology to the radio frequency domain. The substantially longer wavelengths of radio waves, compared to light, introduce substantial difficulties in OAM mode separation, combination, and detection. Conventional RF techniques are ill-equipped to effectively handle the subtle spatial variations associated with OAM modes. This limitation leads to signal losses during transmission and demultiplexing, ultimately reducing the overall link efficiency of the OAM-based communication system [29].

The realization of OAM's transformative potential for communication capacity hinges upon a critical challenge: the development of compact and high-efficiency radio frequency components specifically tailored for OAM applications. Existing designs often suffer from significant power losses, which significantly compromise the overall performance of OAM-based communication systems.

While the potential of OAM to revolutionize communication capacity is undeniable, its realization hinges upon the development of compact and efficient OAM-enabled radio frequency (RF) components [30,31]. Fortunately, the generation of OAM-carrying waves exhibits striking similarities in both the optical and RF domains, with spiral phase plates playing a key role in modulating the wave's phase profile [32].

Despite remarkable advancements in modern communication systems, fundamental challenges remain in enhancing capacity due to limitations in the radio frequency spectrum and polarization. These challenges are further exacerbated by the implementation of sophisticated coding and resource allocation techniques.

In modern communication systems, there is a growing demand for increased transmission capacity in various applications, including backhauls and data centers [33,34]. One approach to achieving higher capacity in a communication link is to transmit multiple independent data streams within a single physical medium or space. The orthogonality of these data streams facilitates efficient multiplexing and demultiplexing at the transmitter and receiver. [35] If the multiplexed data are radiated along a single axis, only one output aperture is required for both transmission and reception. OAM provides a promising solution to this challenge.

OAM is characterized by a helical phase distribution on the wavefront. A set of phase rotations that are integer multiples of $2\pi l$ represent an orthogonal basis set. The phase of the wavefront of an OAM beam is defined as $\exp(il\theta)$, where l is an integer and represents the OAM mode order [36,37].

It is crucial to recognize that angular momentum behaves similarly to other electromagnetic quantities, such as energy and linear momentum.

The angular momentum (J) of an electromagnetic field can be determined using equation (1):

$$J = \int \varepsilon_0 r \times Re\{E \times B^*\} dV \tag{1}$$

The total angular momentum (J) of an electromagnetic field can be decomposed into two components: SAM and OAM. This decomposition, known as the Humblet decomposition, is based on the concept of polarization [38]. Polarization, a classical manifestation of the quantum mechanical concept of spin, generates SAM when it originates from an intrinsic source and OAM when it originates from an extrinsic source.

SAM mode order is denoted by S, while OAM mode order is denoted by l. The total angular momentum, represented by AM, is the combination of these two modes and can be expressed as

$$J = L + S.$$

Equation 2 is used to obtain J:

$$J = \frac{\omega J_z}{\frac{\varepsilon_0}{2}\int(|E|^2 + c^2|B|^2 dV)} \tag{2}$$

The defining characteristic of OAM is the rotation of the phase on the wavefront. This concept should not be confused with polarized beams, in which the electromagnetic field vector is rotating. Distinguishing between OAM and polarization is crucial as they represent distinct physical phenomena with different implications. OAM is associated with the transfer of angular momentum between the wave and matter, while polarization is related to the orientation of the electric field vector and its interaction with polarizable materials.

Figure 1 illustrates different OAM modes, each with a unique helical phase pattern and corresponding OAM value. These helical phase patterns are a defining feature of OAM beams, distinguishing them from other types of electromagnetic waves. As illustrated in Figure 1, all communications to date, employing conventional orthogonalization methods, have been restricted to the zeroth OAM mode. By utilizing other OAM modes simultaneously at the same frequency, this orthogonality can be exploited to transmit significantly more information over a single channel. Efficient frequency utilization by employing OAM modes in radio communication networks holds the potential for a substantial enhancement in spectral efficiency.

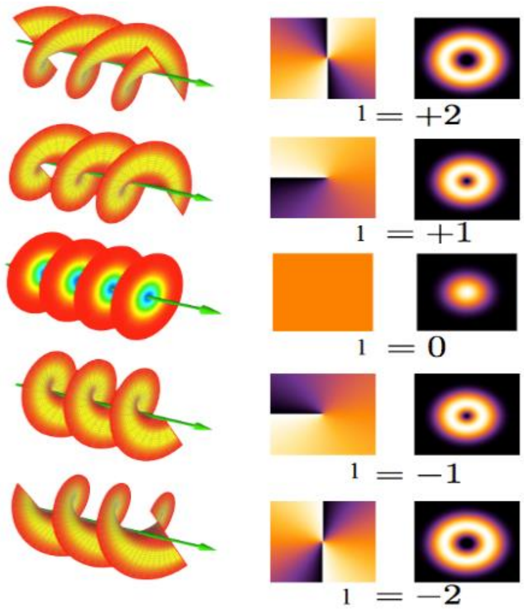

Figure 1 Different OAM modes

The introduction of OAM as an additional orthogonal dimension revolutionizes the landscape of communication possibilities. By leveraging the unique helical phase patterns of OAM modes, multiple independent data streams can be transmitted simultaneously within the same frequency band without interference. This remarkable capability stems from the inherent orthogonality of OAM modes, ensuring that each mode propagates independently without crosstalk with other modes.

The generation, transmission, and measurement of millimeter-wave OAM waves were studied in 1998, and Wi-Fi bands were studied in 2010. The performance of radio links reported in OAM waves is at frequencies of 2.4GHz, 10GHz, 17GHz, 29GHz, 60GHz, and 100GHz with distances exceeding 440 meters.

Several types of electromagnetic wave generators with OAM have been designed so far, the most important of which are circular microstrip antennas [39], reflector antennas with helical algorithms, the use of ring resonators, leaky wave antennas [40], array antennas, and the use of dielectrics in the mouth of a horn antenna [41].

These systems are mainly based on two general methods: the method based on using a circular array of antenna elements, where these elements have the same magnitude and different phases depending on the number of antenna elements, and another method based on using an SPP that creates a helical phase shape.

Recently, due to advancements in technology in the fields of optics and high-speed communications, there has been an increasing tendency among communication engineers worldwide to utilize rotating beams more extensively.

In this paper, three simulation scenarios have been designed to evaluate the performance of OAM antennas with various modes. By analyzing the system's response to different types of interference, including neighboring interference and intentional jamming, we can identify their strengths and weaknesses. This analysis enables us to develop effective strategies to enhance performance and bolster security against jamming. Overall, this approach contributes to a deeper understanding of the capabilities of OAM antennas in real-world conditions and practical applications.

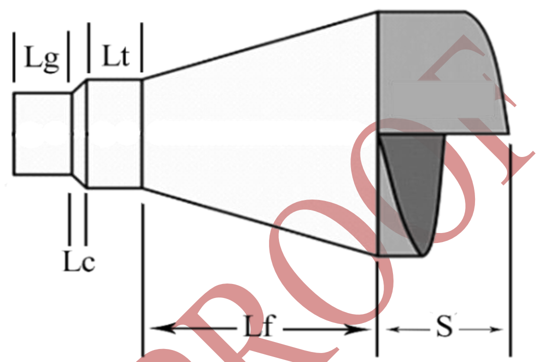

Figure 2 Schematic view of a horn antenna with a spiral phase plane

II. Designing a Horn Antenna with SPP to Generate OAM Beams

The conventional horn antenna is one of the well-known and common antennas as the feed of aperture antennas [42,43]. Due to the wide use of this antenna, extensive research has been done on improving the performance of the horn antenna by adjusting its structure [44].

To generate higher-order OAM modes, here we use a horn antenna with a dielectric in the shape of a spiral circular plate at its output aperture. Figures (2) and (3) depict the schematic of an OAM-carrying wave antenna.

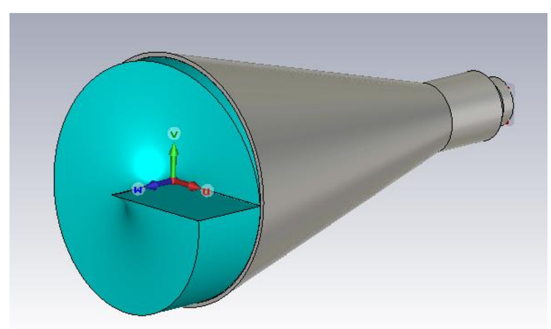

Figure 3 Horn antenna with dielectric plate at 2.4 GHz frequency simulated in CST software

A. Dielectric Plate

The spiral dielectric plate is positioned to create a phase difference of 180 degrees between two points on the plate with equal radius and opposite directions. Discontinuity in the height of the dielectric induces helical phase rotation in the wavefront. Thus, to create a phase difference $\Delta\varphi$ with a wavelength λ based on the azimuthal angle θ with an elevation difference S, we have from equation (3):

$$\psi = \frac{n_1 - n_2}{\lambda} s\varphi \qquad (3)$$

Where n is the refractive index difference between the dielectric and air. Considering that the total azimuthal angle θ is $2\pi l$, and for OAM modes we had l, we can obtain the height of the spiral plate from equation (4).

$$s = \frac{\lambda l}{n_1 - n_2} \tag{4}$$

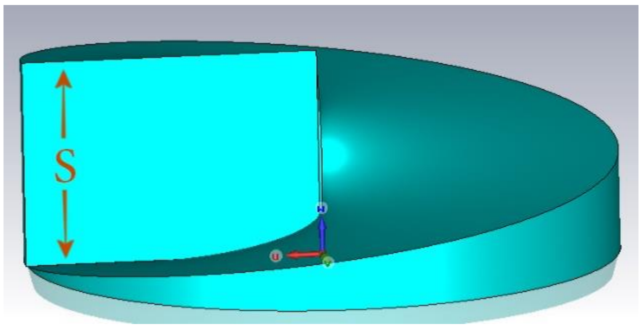

Figure 4 Dielectric plate in the exit opening of the horn antenna

Given the central frequency of 2.4 GHz and the Dielectric permittivity ε_r, we will have the height difference S=23.25mm.

B. Horn Antenna

The wide range of applications and unique features such as suitable bandwidth, low interference from multipath effects, low spillover, and high gain have made horn antennas conducive for various applications. This antenna is fed by a circular waveguide with the TE_{11} mode. This mode can be created using various coaxial-to-waveguide converters. The dimensions of these converters are chosen to support the TM_{11} mode as well. By adjusting the dimensions of the waveguide, the TE_{11} mode can be converted to TM_{11}, resulting in uniform radiation in the antenna aperture.
The presence of the TM_{11} mode, in addition to the dominant TE_{11} mode, reduces the creation of radiation patterns with suitable symmetry in the beam, and minimizes cross-polarization. By creating the appropriate phase at the aperture, the TM_{11} mode causes the H_φ and E_φ components to cancel out.
In a horn antenna, a phase plate is used to create the TM_{11} mode with a step change in the throat of the antenna. However, caution must be exercised in selecting the dimensions to support the TE_{11} mode and ensure that the TM_{11} mode is above the cut-off frequency and does not generate the TE_{21} mode. At the center of the antenna aperture, the two modes reinforce each other, while at the edges, they weaken each other, creating a conical mode in the E and H fields.

By placing a spiral dielectric plate on the aperture, a 180-degree phase difference is created between two points with opposite radii. This delay depends on the azimuthal angle, the refractive indices of the dielectric material, the surrounding environment, and the height of the step created in the dielectric.
The result is a horn antenna with a symmetrical beam with linear polarization and a null in the main field of the antenna pattern. This null is created due to phase rotation in half of the antenna aperture.
Table (1) provides the dimensions of various horn antennas.

Table 1 Horn antenna design parameters

f	Center Frequency	2.4 GHz
L_g	Waveguide Length	41.43 mm
L_t	Transmission size	184.8 mm
L_c	chamfer length	32.10 mm
L_f	Flare size	934.4 mm
S	Dielectric Plate Length	23.25 mm
ε_r	Dielectric permittivity	2.3 mm

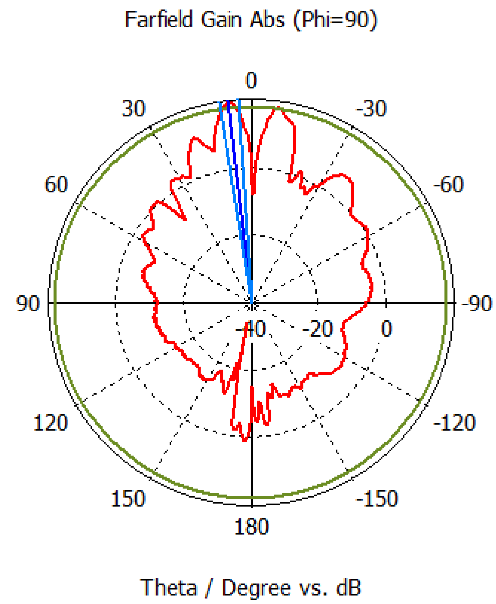

Figure 5 The pattern of the OAM carrier horn antenna, which has a zero in its center

III. The Results of the Simulation

Initially, the most important result needed is the phase rotation in the wavefront, which is the main characteristic of OAM beams, is considered. As shown in Figure (6), the wavefront phase rotates according to equation (3), which is essential for generating the desired mode, and alternates between zero and 360 degrees in rotation.

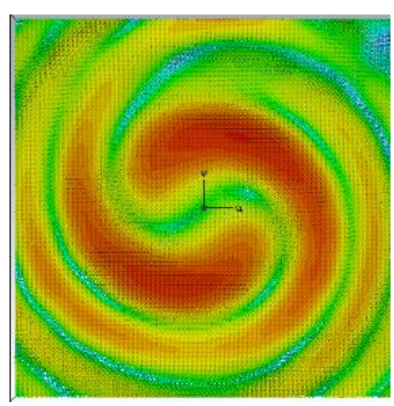

Figure 6 Phase rotation of electric fields

From another perspective, in plane waves, there exists an orthogonality between the electric and magnetic fields, known as the Poynting vector. Because in plane waves, the directions of these fields are always aligned in one direction, the Poynting vector always lies in one direction. The same applies to OAM beams, where the Poynting vector also arises from the orthogonality between the electric and magnetic fields, but with the difference that the electric and magnetic fields are constantly rotating, so this vector also rotates.

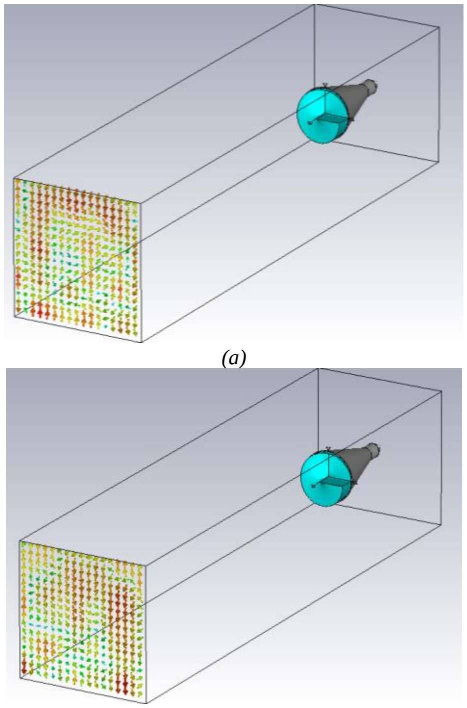

(a)

(b)

Figure 7 E-Field for, (a)mode +2,(b)mode +1.

The reflection coefficient from the antenna aperture is a significant consideration. In a designed antenna, the S-parameter chart represents the standard level of reflection.

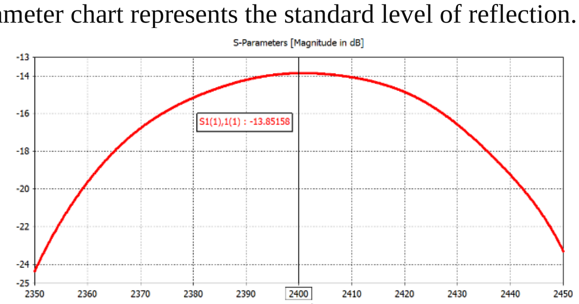

Figure 8 S parameters of horn antenna with spiral phase plane

A. Production of higher-order Modes

In the simulations conducted, we aimed to achieve higher-order modes. Based on equation (4), the height of the spiral phase plate was calculated for each mode, and the results are observed in Figure (9).

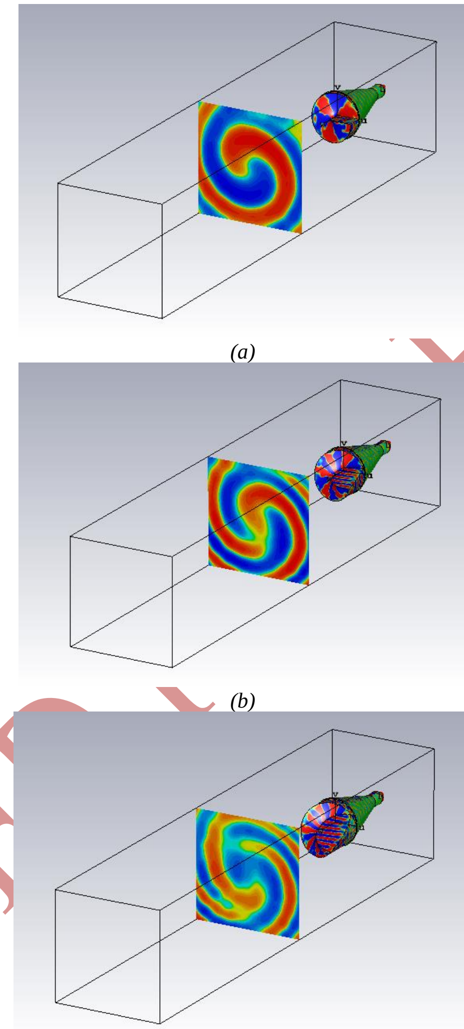

(a)

(b)

(c)

Figure 9 Different OAM modes, (a) S=23.25mm Mode= $+1$, (b) S=46.51mm Mode $l = +2$ and (c) S=66.77mm Mode $l = +3$.

B. Far-field results

Considering the division of antenna regions into near and far fields, and the fact that the behavior of far-field regions is often of interest, simulations were conducted for these regions to compare the results. This aims to prove that the desired results are obtained even in the far-field regions. Equation (5) provides the distance to the far-field regions.

$$d = \frac{2D^2}{\lambda} \quad (5)$$

Given the wavelength $\lambda = 125mm$ and the size of the antenna aperture $D = 66.71mm$, the far-field regions are located at a distance of 7.12 meters from the antenna aperture. As shown in Figure (10), it can be observed that the phase behavior in the far-field regions is consistent with the near-field regions.

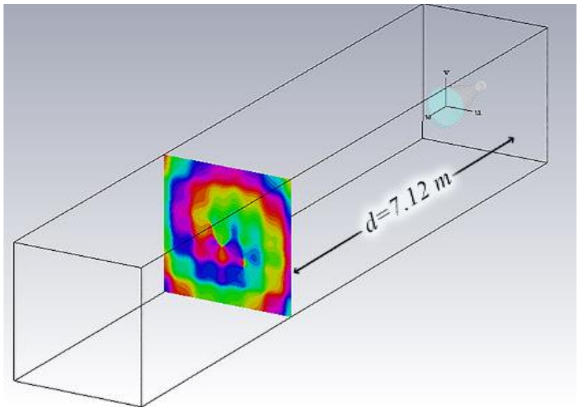

Figure 10 Phase rotation in far fields

C. Comparison of the normal horn antenna (zero order) with the emitting antenna of higher order OAM modes

To compare these two antennas, two parameters, pattern, and phase of the wavefront, are considered. As shown in Figure (11), no phase rotation in the wavefront is observed in a conventional horn antenna.

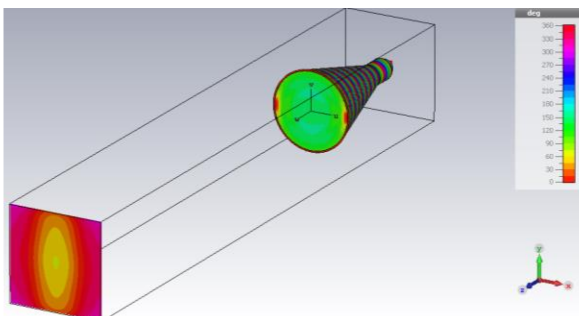

Figure 11 Wave Plate of horn antenna

Now, in Figure (12), the phase rotation in the wavefront of an antenna generating OAM modes is visible.

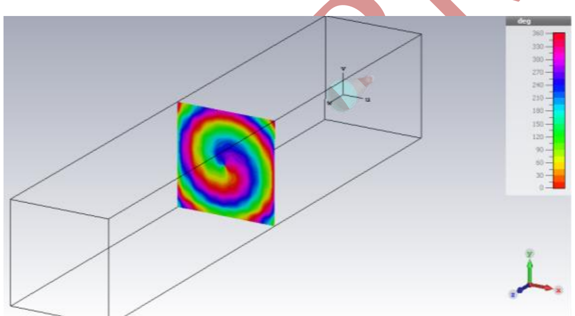

Figure 12 Phase rotation in the wavefront of an OAM antenna

IV. OAM COMMUNICATION LINK

In the design of a communication link, several important parameters are involved, with the primary ones being the transmitter and receiver components. To achieve the desired results regarding OAM-carrying waves, where security and prevention of unauthorized access are paramount, we introduce a communication link in three scenarios. In each scenario, we examine the level of reception. For the implementation of these scenarios, we use a conventional horn antenna and a horn antenna with a spiral phase plate, with the combination of these two antennas as follows.

A. The first scenario: a communication link consisting of two conventional horn antennas

Initially, we observed a link consisting of two conventional horn antennas positioned 10 meters apart from each other. Our expectation from this link is adequate reception due to the uniform conditions of the transmitter and receiver, as depicted in Figure (13).

Given the scatter plot, we can expect the ability to establish communication under balanced conditions.

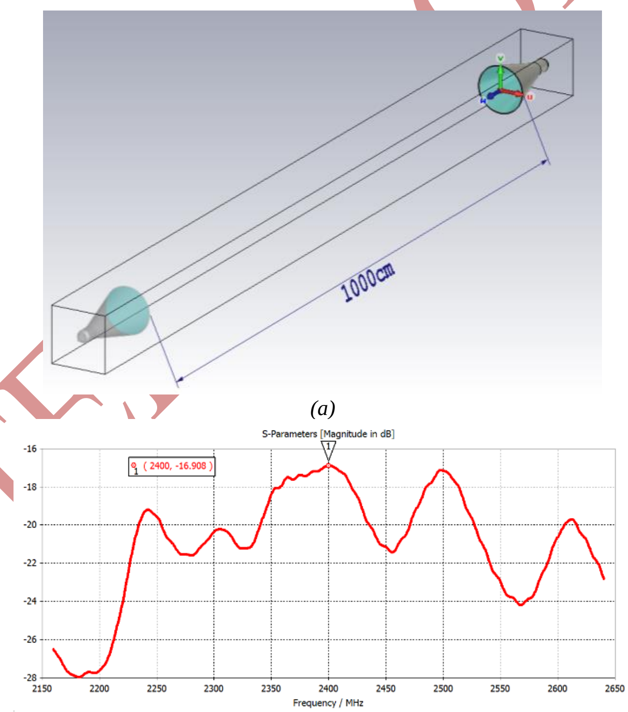

(a)

(b)

Figure 13 Simulation setup of two horn antennas with zero mode, (a) CST Software, (b) Transmission between two antennas.

B. The second scenario: Analysis of the best placement of a jammer or optimal eavesdropping to destroy a communication link

In the second scenario, we considered a communication link between a conventional horn antenna and an OAM carrier wave antenna. This configuration was chosen to demonstrate the selectivity of OAM-based communication systems. By understanding the transmission modes at the sender and receiver, we can highlight the potential for increased security. Our results show that when an OAM carrier wave with mode number +1 is transmitted from the OAM antenna, an ordinary horn antenna (mode 0) is optimally placed directly in front of the transmitter to act as a jammer or eavesdropper. Despite the possibility of maximum degradation in the performance of the communication link in this case, the signal level receives approximately -40 dB, as shown in Figure 14. This significant attenuation indicates that unauthorized receivers, operating with normal mode 0 modes, will have great difficulty in intercepting the transmitted signal. Such a low signal level emphasizes a high level of isolation between the apertures of the conventional horn antenna and the OAM antenna, thereby providing a strong foundation for secure communication links. By reducing the received signal level in the common horn antenna for eavesdroppers or jammers, the anti-eavesdropping and anti-jammer properties of the proposed communication link can be realized.

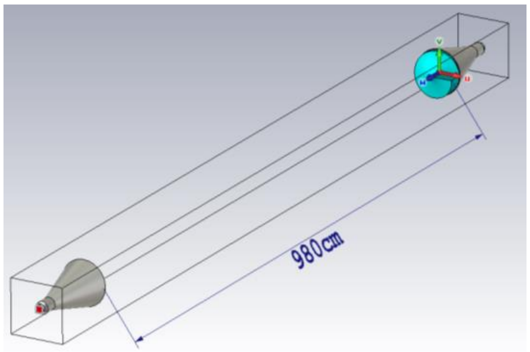

(a)

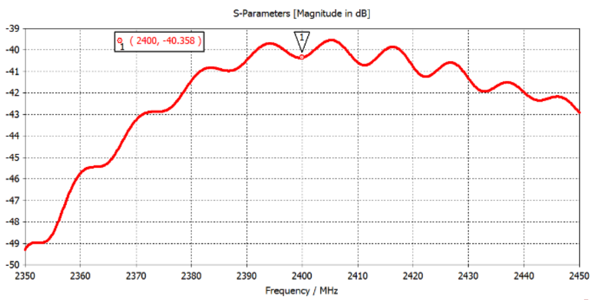

(b)

Figure 14 Simulation setup of two horn antennas with $l = 0$ and $l = +1$ mode, (a) CST Software, (b) Transmission between two antenna.

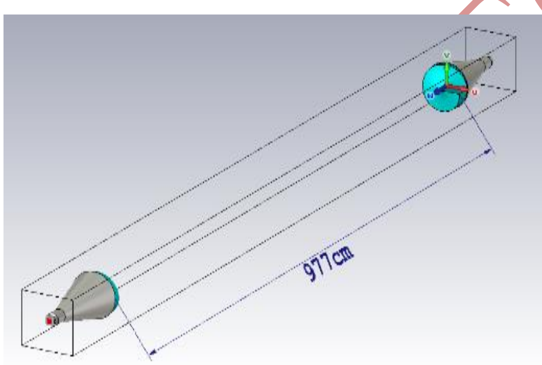

(a)

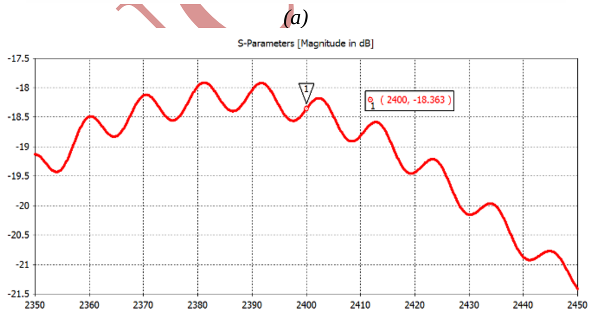

(b)

Figure 15 Simulation setup of two horn antennas with $l = +1$, (a) CST Software, (b) Transmission between two antennae.

C. The third scenario: a communication link consisting of two antennas carrying the OAM wave

In the third scenario, both the transmitter and receiver employ antennas capable of generating and receiving OAM waves. This configuration represents the ideal communication link for our purposes. In this setup, both devices actively participate in establishing a reliable communication channel. To validate the effectiveness of this link, we measured the received signal strength, as illustrated in Figure 15. The results demonstrate that the received signal strength is well within acceptable limits, confirming the feasibility of utilizing OAM waves for practical communication systems. Importantly, this scenario highlights the potential for two antennas operating with +1 OAM modes to function as both the transmitter and receiver in a communication link. Furthermore, a comparison between the first scenario (Figure 13) and the third scenario (Figure 15) reveals a difference of approximately 1.455 dB in the received signal strength. This relatively small difference underscores the viability of employing OAM waves in conventional communication links while offering a substantial enhancement in terms of link security.

Table 2 compares the present research with previous studies in the field of OAM antennas. This table examines key aspects, including simulation scenarios, anti-jamming techniques, and performance metrics for each study.

The results presented indicate that our research, focusing on the design of three distinct simulation scenarios for OAM antennas and the implementation of innovative anti-jamming techniques, significantly emphasizes improving performance and enhancing security against intentional interference.

This comparison demonstrates how the proposed method provides flexibility in generating various OAM modes through the design of different Spiral Phase Plates (SPPs), contributing to a better understanding and optimization of OAM-based communication systems.

Table 2 Comparison of the paper with previous works

Study	Frequency	Gain	Mode Operation	flexibility
[45]	2.4 GHz	3dBi	$L = -1, -2$	No
[46]	2.33 GHz	-	$L = 1\,, 2$	No
[47]	5.5 GHz	10.2dBi	$L = +1\,, -1$	No
[48]	5.8 GHz	8dBi	$L = 0\,, -1, -2, -3$	No
Our work	2.4 GHz	18dBi	$L = +1, +2, +3$	Yes

V. Conclusion

By designing and simulating an SPP Horn antenna, we successfully generated higher-order electromagnetic modes, where the phase rotation of the wavefront became the most significant characteristic of non-zero modes. Through this exploration of higher-order modes, this study has introduced a novel anti-eavesdropping and anti-jamming communication link, capitalizing on the intrinsic security features of Orbital Angular Momentum (OAM) beams. The results of our simulations and analysis indicate that OAM-based systems can offer significant advantages in terms of security, robustness, and capacity compared to conventional communication systems. Our findings pave the way for the development of more secure and reliable wireless communication networks. Moreover, our analysis of scenarios one and two revealed a notable 23.45 dB reduction in jammer signal strength at the receiver in direct-line-of-sight links. This proposed design, with its enhanced security and robustness, is well-suited for point-to-point links in inter-cell communication, making it a promising candidate for future 5G and 6G networks.

References

[1] Wood, Timothy, K. K. Ramakrishnan, Jinho Hwang, Grace Liu, and Wei Zhang. "Toward a software-based network: integrating software-defined networking and network function virtualization." IEEE Network 29, no. 3 (2015): 36-41.

[2] Alladi, Tejasvi, Vinay Chamola, Reza M. Parizi, and Kim-Kwang Raymond Choo. "Blockchain applications for industry 4.0 and industrial IoT: A review." Ieee Access 7 (2019): 176935-176951.

[3] O'Brien, William, Martin Hayes, Mihai Penica, Jeff McCann, Denis Moore, and Eoin O'Connell. "Enabling communications for industry 4.0: Private 5g in smart manufacturing." In 2023 34th Irish Signals and Systems Conference (ISSC), pp. 1-7. IEEE, 2023.

[4] Fotouhi, Azade, Ming Ding, and Mahbub Hassan. "DroneCells: Improving spectral efficiency using drone-mounted flying base stations." Journal of Network and Computer Applications 174 (2021): 102895.

[5] Shaik, Nilofer, and Praveen Kumar Malik. "A comprehensive survey 5G wireless communication systems: open issues, research challenges, channel estimation, multi-carrier modulation, and 5G applications." Multimedia Tools and Applications 80, no. 19 (2021): 28789-28827.

[6] Zhang, Haiyang, Nir Shlezinger, Francesco Guidi, Davide Dardari, and Yonina C. Eldar. "6G wireless communications: From far-field beam steering to near-field beam focusing." IEEE Communications Magazine (2023).

[7] Anand, Rohit, Shahanawaj Ahamad, Vivek Veeraiah, Sushil Kumar Janardan, Dharmesh Dhabliya, Nidhi Sindhwani, and Ankur Gupta. "Optimizing 6G wireless network security for effective communication." In Innovative Smart Materials Used in Wireless Communication Technology, pp. 1-20. IGI Global, 2023.

[8] Zhou, Gui, Cunhua Pan, Hong Ren, Kezhi Wang, and Zhangjie Peng. "Secure wireless communication in RIS-aided MISO system with hardware impairments." IEEE Wireless Communications Letters 10, no. 6 (2021): 1309-1313.

[9] F. Tamburini, B. Thid, E. Mari, A. Spinelli, A. Bianchini, and F. Romanato, "Reply to comment on 'Encoding many channels on the same frequency through radio vorticity: First experimental test,'" New J. Phys., vol. 14, 2012.

[10] You, Xiaohu, Cheng-Xiang Wang, Jie Huang, Xiqi Gao, Zaichen Zhang, Mao Wang, Yongming Huang, et al. "Towards 6G wireless communication networks: Vision, enabling technologies, and new paradigm shifts." Science China Information Sciences 64 (2021): 1-74.

[11] Yuan, Xiaojun, Ying-Jun Angela Zhang, Yuanming Shi, Wenjing Yan, and Hang Liu. "Reconfigurable-intelligent-surface empowered wireless communications: Challenges and opportunities." IEEE Wireless Communications 28, no. 2 (2021): 136-143.

[12] Amiri, I. S., Ahmed Nabih Zaki Rashed, Abd Elnaser A. Mohammed, Ehab Salah El-Din, and P. Yupapin. "Spatial continuous wave laser and spatiotemporal VCSEL for high-speed long haul optical wireless communication channels." Journal of Optical Communications 44, no. 1 (2023): 43-51.

[13] Jamshed, Muhammad Ali, Kamran Ali, Qammer H. Abbasi, Muhammad Ali Imran, and Masood Ur-Rehman. "Challenges, applications, and future of wireless sensors in the Internet of Things: A review." IEEE Sensors Journal 22, no. 6 (2022): 5482-5494.

[14] Ebadi, Seyed Morteza, Shiva Khani, and Jonas Örtegren. "Design of miniaturized wide band-pass plasmonic filters in MIM waveguides with tailored spectral filtering." *Optical and Quantum Electronics* 56, no. 5 (2024): 1-24.

[15] Xu, Hanyue, Ying Wang, Farhan A. Ghaffar, and Langis Roy. "Reconfigurable microwave filters implemented using field programmable microwave substrate." *IEEE Transactions on Microwave Theory and Techniques* 69, no. 2 (2020): 1344-1354.

[16] Ebadi, Seyed Morteza, and Shiva Khani. "Highly-miniaturized nano-plasmonic filters based on stepped impedance resonators with tunable cut-off wavelengths." *Plasmonics* 18, no. 4 (2023): 1607-1618.

[17] Hagelauer, Amelie, Rich Ruby, Shogo Inoue, Victor Plessky, Ken-Ya Hashimoto, Ryo Nakagawa, Jordi Verdu, et al. "From microwave acoustic filters to millimeter-wave operation and new applications." *IEEE Journal of Microwaves* 3, no. 1 (2022): 484-508.

[18] Khani, Shiva, Mohammad Danaie, Pejman Rezaei, and Ali Shahzadi. "Compact ultra-wide upper stopband microstrip dual-band BPF using tapered and octagonal loop resonators." *Frequenz* 74, no. 1-2 (2020): 61-71.

[19] Xu, Xingyuan, Mengxi Tan, Jiayang Wu, Andreas Boes, Bill Corcoran, Thach G. Nguyen, Sai T. Chu et al. "Photonic RF and microwave integrator based on a transversal filter with soliton crystal microcombs." *IEEE Transactions on Circuits and Systems II: Express Briefs* 67, no. 12 (2020): 3582-3586.

[20] Khani, Shiva, Mohammad Danaie, and Pejman Rezaei. "Realization of single-mode plasmonic bandpass filters using improved nanodisk resonators." *Optics Communications* 420 (2018): 147-156.

[21] L. Allen, M. W. Beijersbergen, R. J. C. Spreeuw, and J. P. Woerdman, "Orbital angular momentum of light and the transformation of Laguerre-Gaussian laser modes," *Phys. Rev. A*, vol. 45, no. 11, pp. 8185–8189, 1992.

[22] Y. Yan, G. Xie, M. P. J. Lavery, H. Huang, N. Ahmed, C. Bao, Y. Ren, Y. Cao, L. Li, Z. Zhao, A. F. Molisch, M. Tur, M. J. Padgett, and A. E. Willner, "High-capacity millimeter-wave communications with orbital angular momentum multiplexing.," Nat. Commun., vol. 5, p. 4876, 2014.

[23] M. J. Strain, X. Cai, J. Wang, J. Zhu, D. B. Phillips, L. Chen, M. Lopez-Garcia, J. L. O'Brien, M. G. Thompson, M. Sorel, and S. Yu, "Fast electrical switching of orbital angular momentum modes using ultra-compact integrated vortex emitters," Nat. Commun., vol. 5, p. 4856, 2014

[24] J. Wang, J.-Y. Yang, I. M. Fazal, N. Ahmed, Y. Yan, H. Huang, Y. Ren, Y. Yue, S. Dolinar, M. Tur, and A. E. Willner, "Terabit free-space data transmission employing orbital angular momentum multiplexing," Nat. Photonics, vol. 6, no. 7, pp. 488–496, 2012.

[25] N. Bozinovic, Y. Yue, Y. Ren, M. Tur, P. Kristensen, H. Huang, A. E. Willner, and S. Ramachandran, "Terabit-Scale Orbital Angular Momentum Mode Division Multiplexing in Fibers," Science (80-.)., vol. 340, no. 6140, pp. 1545–1548, 2013.

[26] S. M. Mohammadi, L. K. S. Daldorff, J. E. S. Bergman, R. L. Karlsson, B. Thide, K. Forozesh, T. D. Carozzi, and B. Isham, "Orbital Angular Momentum in Radio;A System Study," IEEE Trans. Antennas Propag., vol. 58, no. 2, pp. 313–572, 2010

[27] Feng, Qiang, Xudong Kong, Mingming Shan, Yifeng Lin, Long Li, and Tie Jun Cui. "Multi-orbital-angular-momentum-mode vortex wave multiplexing and demultiplexing with shared-aperture reflective metasurfaces." Physical Review Applied 17, no. 3 (2022): 034017.

[28] Siyad, C. Ismayil, and S. Tamilselvan. "Deep learning enabled physical layer security to combat eavesdropping in massive MIMO networks." In Second International Conference on Computer Networks and Communication Technologies: ICCNCT 2019, pp. 643-650. Springer International Publishing, 2020.

[29] Willner, Alan E., Yongxiong Ren, Guodong Xie, Yan Yan, Long Li, Zhe Zhao, Jian Wang, Moshe Tur, Andreas F. Molisch, and Solyman Ashrafi. "Recent advances in high-capacity free-space optical and radio-frequency communications using orbital angular momentum multiplexing." Philosophical Transactions of the Royal Society A: Mathematical, Physical and Engineering Sciences 375, no. 2087 (2017): 20150439.

[30] A. Habibi Daronkola, F. Tavakol Hamedani, P. Rezaei, A. Pesarakloo, S. A. Khatami, “Studying superposition of multiple OAM modes for beam concentration using circular arrays for long-range communication,” International Journal of RF and Microwave Computer-Aided Engineering, vol. 32, no. 11, 23331, November 2022.

[31] A. Habibi Daronkola, F. Tavakkol Hamedani, P. Rezaei, N. Montaseria, “Mutual coupling reduction using plane spiral orbital angular momentum electromagnetic wave,” Journal of Electromagnetic Waves and Applications, vol. 36, no. 3, pp. 346-355, 2022.

[32] X.-L. Cai, J.-W. (University of B. Wang, M. J. Strain, B. Johnson-Morris, J.-B. Zhu, M. Sorel, J. L. O’Brien, M. G. Thompson, and S.-Y. Yu, “Integrated Compact Optical Vortex Beam Emitters,” Science (80-.)., vol. 338, no. 6105, pp. 363–366, 2012

[33] L. Cheng, W. Hong, and Z.-C. Hao, “Generation of electromagnetic waves with arbitrary orbital angular momentum modes.,” Sci. Rep., vol. 4, p. 4814, 2014

[34] S. Hur, T. Kim, D. J. Love, J. V. Krogmeier, T. A. Thomas and A. Ghosh, "Millimeter Wave Beamforming for Wireless Backhaul and Access in Small Cell Networks," in IEEE Transactions on Communications, vol. 61, no. 10, pp. 4391-4403, October 2013.

[35] Y. Katayama, K. Takano, Y. Kohda, N. Ohba, D. Nakano, “Wireless data center networking with steered-beam mmWave links,” IEEE Wireless Communications and Networking Conference, 2011, pp. 2179–2184.

[36] Ren, Yongxiong, Long Li, Zhe Wang, Seyedeh Mahsa Kamali, Ehsan Arbabi, Amir Arbabi, Zhe Zhao, et al. "Orbital angular momentum-based space division multiplexing for high-capacity underwater optical communications." Scientific Reports 6, no. 1 (2016): 33306.

[37] Lei, Ting, and Xiaocong Yuan. "Orbital angular momentum (OAM) based optical routing using reconfigurable optical vortex grating." In CLEO: Science and Innovations, pp. SW4F-4. Optica Publishing Group, 2016.

[38] A. F. Molisch, “Wireless communications,” books.google.com, 2011.

[39] Chashmi, Mohsen Jafari, Pejman Rezaei, Amir Hossein Haghparast, and Davoud Zarifi. "Dual circular polarization 2× 2 slot array antenna based on printed ridge gap waveguide technology in Ka-band." AEU-International Journal of Electronics and Communications 157 (2022): 154433.

[40] P. Sohrabi, P. Rezaei, S. Kiani, M. Fakhr, “A symmetrical SIW-based leaky-wave antenna with continuous beam scanning from backward-to-forward through broadside,” Wireless Networks, vol. 27, pp. 5417-5424, 2021.

[41] A. Amne Elahi, P. Rezaei, “Axial corrugated horn antenna with elliptical tapering function,” Journal of Electrical and Computer Engineering Innovations, vol. 5, no. 1, pp. 1-5, 2017.

[42] S.H. Ramazannia Tuloti, P. Rezaei, F. Tavakkol Hamedani, “Unit-cell with flexible transmission phase slope for ultra-wideband transmitarray antennas,” IET Microwaves, Antennas & Propagation, vol. 13, no. 10, pp. 1522-1528, 2019.

[43] S.H. Ramazannia Tuloti, P. Rezaei, F. Tavakkol Hamedani, “High-efficient wideband transmitarray antenna,” IEEE Antennas and Wireless Propagation Letters, vol. 17, no. 5, pp. 817-820, 2018.

[44] A.H. Haghparast, P. Rezaei, “High-performance H-plane horn antenna using groove gap waveguide technology,” AEU International Journal of Electronics and Communications, vol. 163, 154620, 2023.

[45] Guo, Chong, Xunwang Zhao, Cheng Zhu, Peng Xu, and Yu Zhang. "An OAM patch antenna design and its array for higher order OAM mode generation." *IEEE Antennas and Wireless Propagation Letters* 18, no. 5 (2019): 816-820.

[46] Liu, Dandan, Liangqi Gui, Zixiao Zhang, Han Chen, Guochao Song, and Tao Jiang. "Multiplexed OAM wave communication with two-OAM-mode antenna systems." *IEEE Access* 7 (2018): 4160-4166.

[47]Li, Hui, Le Kang, Feng Wei, Yuan-Ming Cai, and Ying-Zeng Yin. "A low-profile dual-polarized microstrip antenna array for dual-mode OAM applications." *IEEE Antennas and Wireless Propagation Letters* 16 (2017): 3022-3025.

[48] Qin, Fan, Lihong Li, Yi Liu, Wenchi Cheng, and Hailin Zhang. "A four-mode OAM antenna array with equal divergence angle." *IEEE Antennas and Wireless Propagation Letters* 18, no. 9 (2019): 1941-1945.